


Research Article

Super-Resolution Reconstruction Algorithm-Based MRI Diagnosis of Prostate Cancer and Evaluation of Treatment Effect of Prostate Specific Antigen

Biao Liu,¹ Rongping Tan,¹ Baogao Tan,¹ Chenhui Huang,¹ and Keqin Yang ²

¹Department of Radiology, Guigang People's Hospital, Guigang 537100, Guangxi, China

²Department of Orthopaedics, Guigang People's Hospital, Guigang 537100, Guangxi, China

Correspondence should be addressed to Keqin Yang; 2011151110@hbut.edu.cn

Received 25 August 2022; Revised 24 September 2022; Accepted 28 September 2022; Published 15 October 2022

Academic Editor: Enas Abdulhay

Copyright © 2022 Biao Liu et al. This is an open access article distributed under the Creative Commons Attribution License, which permits unrestricted use, distribution, and reproduction in any medium, provided the original work is properly cited.

MRI of prostate cancer (PCa) was performed using a projection onto convex sets (POCS) super-resolution reconstruction algorithm to evaluate and analyze the treatment of prostate-specific antigen (PSA) and provide a theoretical reference for clinical practice. A total of 110 patients with PCa were selected as the study subjects. First, the modified POCS algorithm was used to reconstruct the MRI images, and the gradient interpolation algorithm was used instead of the traditional bilinear algorithm to preserve the edge information. The diagnostic and therapeutic effects of MRI examination, PSA examination, and MRI combined with PSA based on a super-resolution reconstruction algorithm were then compared. The simulation results showed that the POCS algorithm was superior to the bilinear interpolation results and was superior to the common POCS algorithm. After adding noise artificially, the restoration algorithm was effective and could preserve the details in the image. The performance indexes of PSA in the diagnosis of PCa were 75.4%, 60.1%, 70.08%, 72.2%, and 60.3%, respectively; the performance indexes of MRI in the diagnosis of PCa were 84.6%, 61.4%, 71.11%, 73.08%, and 61.9%, respectively; and the performance indexes of MRI combined with PSA based on the super-resolution reconstruction algorithm in the diagnosis of PCa were 96.05%, 88.3%, 95.1%, 93.6%, and 92.7%, respectively. The indicators of MRI combined with PSA based on the super-resolution reconstruction algorithm were significantly higher than those of the other two methods ($P < 0.05$). The signal-to-noise ratio of MRI of PCa based on the super-resolution reconstruction algorithm has been greatly improved, with good clarity, which can improve the diagnostic accuracy of PCa patients and has certain advantages in the examination. MRI based on the super-resolution reconstruction algorithm has a high value in the diagnosis and treatment of PCa.

1. Introduction

Prostate cancer (PCa) is one of the most common malignant tumors threatening the life safety of men, and worldwide, the incidence of PCa ranks second among male malignant tumors [1]. Although the incidence of PCa is currently low in China, the incidence of the disease in China has shown a significant increase in recent years [2]. With the increasing aging of the population in China, as well as the gradual hyper-lipidation of dietary patterns and the popularization of examinations in elderly men, the incidence of the disease remains an increasing possibility [3]. For the determination of PCa diagnosis and treatment options as well as its

prognosis, the early diagnosis of tumors and the clinical staging of tumors play a decisive role. For lesions localized in the capsule, radical PCa resection is one of the effective treatments for the disease [4]. At present, prostate biopsy remains the gold standard for preoperative examination of PCa in China, but this examination method is not applicable to patients with smaller lesions because the lesions are limited by the number of puncture needles when they are small, and the diseased tissue cannot be removed, resulting in low sensitivity. The results of relevant clinical studies showed that the missed diagnosis rate of needle biopsy was about 30% [5]. In addition, most elderly patients are not well tolerated and accepted for the examination, resulting in a

low proportion of patients receiving puncture techniques and their clinical popularity. At present, MRI and prostate specific antigen (PSA) are the main noninvasive methods used for PCa, but there are differences in the sensitivity and specificity of various examination techniques. PSA is a serine protease secreted by prostate epithelial cells that is significantly present in both normal and abnormal prostate tissues, so PSA can be used as a sensitive indicator for PCa examination [6]. The normal range of this index is 0~4 ng/mL. BPH is predominant in patients with PSA < 4.0 ng/mL, and PCa is predominant in patients with PSA > 10 ng/mL. Overall, PSA values are positively correlated with the incidence of PCa, and this index has now become a commonly used indicator for the diagnosis of PCa [7]. However, PSA is used as a prostate specific indicator rather than a specific indicator of PCa. It is therefore nonspecific in diagnosing PCa. Prostatic hyperplasia, prostatitis, acute urinary retention, and cystoscopy can cause PSA increase. Moreover, a significant disadvantage of the PSA test is the inability to stage PCa.

In recent years, with the gradual application of high-field MRI, rectal coil, body coil, and other techniques in clinical practice, the prostate results can be clearly visualized on MRI T2W1 sequence and hypointense nodules located in the peripheral zone can be sensitively detected, so its sensitivity and specificity in the diagnosis of PCa have been significantly improved. The sensitivity can reach 70%~90%, and the accuracy of diagnosis is also significantly higher than that of ultrasound and CT. However, the results of current clinical studies have shown that some benign diseases such as prostatitis and PIN will also show the central zone in the T2WI sequence of MRI, and hypointense areas will appear in the hyperintense peripheral zone [8]. It has led to decreased sensitivity and specificity of MRI for the diagnosis of PCa. In recent years, MRI technology has been continuously developed, and new technologies such as DCE-MRI have been gradually developed. However, some scholars believe that the sensitivity and specificity of DCE-MRI in the diagnosis of PCa should be further studied and confirmed. There are many reports on MRI and MRD in the diagnosis of prostate cancer, and studies have found that MRI-guided prostate biopsy technique has a significant role in increasing the positive rate of repeated puncture [9]. Overall, the sensitivity and specificity of MRI or PSA alone in the diagnosis of PCa are not too high.

Although MRI has been widely used in clinical practice, however, its disadvantages are also obvious, for example, compared with other imaging methods, the imaging speed of MRI is significantly slower, which leads to an examination time of 15 minutes to an hour or even longer. Maintaining a maneuver for a long time in a closed environment is difficult for some patients, especially elderly and pediatric patients. In addition, high-resolution images can hardly be obtained in the case of movement, so their scanning speed must be fast to avoid artifacts in the case of movement, and if the patient and the examiner cooperate improperly, they need to be re-examined [10, 11]. How to improve the image quality and resolution after acquisition has become the focus of researchers' attention. Super-resolution technology has been

widely used and popularized in astronomy, medical imaging, monitoring, and detection. Traditional super-resolution reconstruction techniques for single images are defined as observing and recovering high-resolution images (HR) from low-resolution images (LR). The results of subsequent related studies showed that the algorithm was greatly affected by noise, and the reconstructed images were less effective [12]. Therefore, this algorithm has not been widely popularized, but it is helpful to the research of super-resolution algorithms. After continuous development and progress, ultrasonic resolution technology has also been greatly developed and advanced. The projection onto convex sets (POCS) algorithm has been widely used and has achieved good results. Some scholars use the POCS algorithm to input the super-resolution algorithm of cardiac images. In this experiment, three-dimensional super-resolution images were reconstructed by using multiple low-resolution two-dimensional cardiac MRI images. This algorithm can not only be used for cardiac MRI image reconstruction but can also be applicable to other anatomical structures [13]. There are many similar related studies, but there are few studies and analyses for PCa.

This study was aimed at investigating the value of MRI and PSA techniques in PCa based on super-resolution reconstruction algorithms in prostate diagnosis. PCa patients were selected as the study subjects to compare MRI examination, PSA examination, and MRI combined with PSA diagnosis and treatment based on super-resolution reconstruction algorithms. It was to provide a reference and basis for the treatment of related diseases in clinical practice.

2. Materials and Methods

2.1. Subjects. A total of 110 PCa patients who visited the hospital from March 2020 to March 2021 were selected as the study subjects. There were 56 male patients and 54 female patients, with a mean age of 66.3 ± 12.8 years. Informed consent was obtained from patients and this study was approved by the ethics committee of the hospital.

2.1.1. Inclusion Criteria. Patients with suspected prostate lesions or abnormal serum PSA were identified by digital rectal examination and B-ultrasonography; patients' age ranged from 35 to 80 years; patients' education level was primary school or above; patients had no communication barriers and were able to communicate normally with researchers.

2.1.2. Exclusion Criteria. Patients with visual acuity or reading and writing disorders; Patients with clinical diagnosis of mental illness; Patients with other serious physical or organ function diseases; Patients with a history of prostate-related surgery.

2.2. Test Methods

2.2.1. PSA Examination. All patients underwent fasting venous blood sampling. Digital rectal examination, catheterization, cystoscopy, prostate biopsy, and other examinations should be avoided before blood collection.

2.2.2. MRI Examination. A 3.0 T MRI scanner was used and placed in the body phased array coil, and axial and coronal fat-compression fast spin echo T2WI scans were performed locally in the prostate, and pelvic midsagittal T1WI scans were performed. Magnetic resonance perfusion imaging was performed: scan parameters were: TR 4.0 ms, TE 1.4 ms, using the fat suppression technique; flip angle 90°; matrix 203 × 320; FOV 317 × 350; slice thickness 2 mm; slice distance 0 mm. A high-pressure syringe was used to inject contrast medium Gd-DTPA at a flow rate of 1.5 mL/s through the cubital vein at a dose of 0.2 mol/kg, and the injection time was 1 to 2 stages from the beginning of the scan, with a scanning time of 13 to 16 s in each stage, for a total of 30 stages of the scan. The obtained images were processed using the software system.

2.3. Image Processing and Analysis. The POCS algorithm is used to reconstruct the MRI image. The image reconstruction mainly includes four parts: the feature extraction and enhancement module; the information refinement module; the fusion reconstruction; and the loss function. The specific details are as follows:

2.3.1. Feature Extraction and Enhancement Module. It is supposed C_1 and C_3 represent the convolution function with size of 1×1 and 3×3 , R represents the ReLU function, O_C^i represents the convolution output of the layer i , O_i represents the output of the layer i , and $O_C^1 = C_3(I_{SR}), O_1 = R(O_C^1)$. The subsequent convolution output representation is shown in the following equation.

$$O_C^i = \begin{cases} C_3(O_{i-1}), & i \text{ is odd number} \\ C_1(O_{i-1}), & i \text{ is even number} \end{cases}. \quad (1)$$

$i \in (2, 17)$ represents the layer index. The output representation of each layer is shown in the following equation.

$$O_j = \begin{cases} R\left(O_C^j + \sum_{j=1}^{j=2} O_C^j\right), & j \text{ is odd number} \\ R(O_C^j), & j \text{ is even number} \end{cases}. \quad (2)$$

$j \in (2, 17)$, the expression method of feature extraction and enhancement module output is shown in the following equation.

$$O_{17} = R\left(O_C^{17} + \sum_{j=1}^{15} O_C^j\right). \quad (3)$$

“+” means residual learning, and O_{17} will eventually be input into the informatization module.

2.3.2. Information Refinement Module. In the initial stage, in order to optimize the input feature F_{in}^t with the feedback information F_{in}^{t-1} , F_{in}^t and F_{out}^{t-1} are spliced and compressed to generate the refined initial feature L_0^t by $\text{Conv}(1, m)$, as shown in the following equation.

$$L_0^t = C_0(F_{out}^{t-1}, F_{in}^t). \quad (4)$$

C_0 is the initial compression operation, $(F_{out}^{t-1}, F_{in}^t)$ indicates the splicing of F_{out}^{t-1} and F_{in}^t . It is assumed that LR and HR characteristic maps are given by the g characteristic mapping structure of the t iteration, and the H_g^t representation method of the HR characteristic map is shown in the following equation.

$$H_g^t = G_g^\uparrow(L_0^t, L_1^t, \dots, L_{g-1}^t). \quad (5)$$

G_g^\uparrow indicates that the down-sampling operation is performed using $\text{Deconv}(k, m)$ in the g feature mapping structure. The representation method of the characteristic diagram L_g^t corresponding to LR is shown in the following equation.

$$L_g^t = G_g^\downarrow(H_1^t, H_2^t, \dots, H_g^t). \quad (6)$$

G_g^\downarrow indicates that the down-sampling operation is performed using $\text{Conv}(k, m)$ in the g feature mapping structure.

In order to make full use of the structural information of each feature map, it fuses the feature LR generated by the feature map structure, and the output of the generated information refinement module is as follows:

$$F_{out}^t = C_{FF}^t(L_1^t, L_2^t, \dots, L_G^t). \quad (7)$$

C_{FF}^t means the function of $\text{Conv}(1, m)$.

2.3.3. Fusion and Reconstruction Module. The expression method of feature fusion process is as follows:

$$O_{RB} = R(O_1 + F_{out}^t), \quad (8)$$

O_1 and F_{out}^t represent the low-level feature and the high-level feature, respectively, and O_{RB} indicates the output of fast information fusion.

The function description of the reconstruction module is as follows:

$$O_{SR} = C_3(R(C_3(R(C_3(R(C_3(O_{RB}))))))). \quad (9)$$

Loss function: the L1 loss function is selected to optimize the network model. The specific network loss function is as follows:

$$L(\theta) = \frac{1}{T} \sum_{i=0}^T \|I_{HR}^t - I_{SR}^t\|. \quad (10)$$

T represents the total number of iterations, I_{HR}^t represents the label of the LR image input in the t iteration, and I_{SR}^t represents the reconstructed image generated in the t iteration.

2.4. Evaluation of Image Reconstruction Effect. Peak signal-to-noise ratio (PSNR) and structural similarity (SSIM) were used to evaluate the performance of the algorithm. PSNR evaluates the image reconstruction quality by calculating the pixel difference between images. The specific principle is as follows:

$$\text{MSE} = \frac{1}{mn} \sum_{i=0}^{m-1} \sum_{j=0}^{n-1} (X(i, j), Y(i, j))^2, \quad (11)$$

$$\text{PSNR} = 10 \log_{10} \left(\frac{(2^k - 1)^2}{\text{MSE}} \right).$$

The calculation method of SSIM is as follows:

$$l(X, Y) = \frac{2\mu_X\mu_Y + C_1}{\mu_X^2 + \mu_Y^2 + C_1}, \quad (12)$$

$$c(X, Y) = \frac{2\sigma_X\sigma_Y + C_2}{\sigma_X^2 + \sigma_Y^2 + C_2}, \quad (13)$$

$$s(X, Y) = \frac{\sigma_{XY} + C_3}{\sigma_X\sigma_Y + C_3}, \quad (14)$$

$$\text{SSIM}(X, Y) = l(X, Y) \cdot c(X, Y) \cdot s(X, Y). \quad (15)$$

2.5. Statistical Methods. SPSS 22.0 statistical software was used for data analysis. Measurement data were expressed as mean \pm standard deviation ($\bar{x} \pm s$). The t -test was used for comparison between groups. Analysis of variance was used for comparison within groups. The χ^2 test was used for enumeration data. $P < 0.05$ was considered statistically significant.

3. Results

3.1. Patient's MRI Image. MRI images of patients before and after processing are shown in Figure 1. Compared with the original image, the image quality of MRI images processed by high-resolution reconstruction algorithm was significantly improved; the image sharpness was also increased; and the edge characteristics; and details of the lesion were clearer and more prominent.

3.2. Evaluation Results of Algorithm Reconstruction Performance. The evaluation results of the image reconstruction quality of traditional image processing techniques and the proposed algorithm are shown in Figures 2 and 3. The PSNR and SSIM values of the traditional algorithm were 22.3 and 0.735, respectively, and the PSNR and SSIM values of the proposed algorithm were 28.6 and 0.89, respectively. It can be found that the proposed algorithm performed significantly better than the traditional algorithm.

3.3. Judgment of PCa Results by Different Diagnostic Methods. The results of different diagnostic methods for PCa are judged as shown in Figures 4–6. Analysis of Figures 4–6 showed that the performance indicators of PSA in the diagnosis of PCa were 75.4%, 60.1%, 70.08%, 72.2%, and 60.3%, respectively; the performance indicators of MRI in the diagnosis of PCa were 84.6%, 61.4%, 71.11%, 73.08%, and 61.9%, respectively; and the performance indicators of MRI combined with PSA based on super-resolution reconstruction algorithm in the diagnosis of PCa were 96.05%, 88.3%, 95.1%, 93.6%, and 92.7%, respectively. The indicators

of MRI combined with PSA based on the super-resolution reconstruction algorithm were significantly higher than those of the other two methods (Figure 7).

4. Discussion

PCa, is a highly prevalent and common malignant tumor disease in men in Europe and the United States. Globally, PCa has the second highest incidence among all male malignancies [14]. In the US, PCa has surpassed lung cancer as the biggest threat to men's health in cancer rankings that threaten men's health. Although its incidence in China is lower than that in Europe and the United States, it has shown a significant increase in recent years and has become the third most important malignant tumor threatening male health after male urinary and reproductive system tumors [15]. In half of the cases, PCa progresses more slowly and the clinical symptoms are very insignificant. In addition, the disease is often easily misdiagnosed as benign prostatic hyperplasia, which leads to delayed diagnosis and treatment. It leads to missed timing of radical prostatectomy. In summary, it has a very important role and significance for the early diagnosis of PCa treatment. In recent years, PSA and MRI technology have developed rapidly and have been widely used in multiple disease areas. The above two techniques are also of great help and advancement for the diagnosis of PCa [16].

PSA is a serine protease secreted by prostate tissue. Currently, its criteria for PCa diagnosis are RPSA > 10 ng/mL for PCa and RPSA < 10 ng/mL for prostate cancer hyperplasia [17, 18]. In general, PSA is characterized by high sensitivity and low specificity for the diagnosis of PCa. The gray zone of PSA detection is $4 \text{ ng/mL} < \text{PSA} < 10 \text{ ng/mL}$, and the overlap zone between benign prostatic hyperplasia and PCa is large. In general, PSA is specific for prostate tissue but not for PCa. It has some impact on the accuracy and sensitivity of PSA for the diagnosis of PCa [19]. PSA was applied to diagnose PCa. The results showed that the negative predictive value, positive predictive value, accuracy, specificity, and sensitivity of PCa were 75.4%, 60.1%, 70.08%, 72.2%, and 60.3%, respectively. It can be found that its performance is general in PCa diagnosis.

MRI can provide physiological, pathological, biochemical, and anatomical information about the prostate. It has high sensitivity for both diagnosis and staging of PCa. This method is considered to be the most effective and ideal noninvasive test for PCa. MRI can quantitatively measure and display the characteristics of water molecules in the microscopic water environment in tissues, thus further providing information on tissue spatial results, so it has the advantages of multi-directional imaging and good tissue resolution [20]. Therefore, it has high application value and potential in the detection of tiny lesions, differentiation of benign and malignant tumors, tumor staging, and helping doctors develop scientific and effective treatment plans. However, MRI also has deficiencies, such as significant changes in metabolic information in patients who have undergone digital examination of tissues and organs, and therefore MRI is clearly not applicable to such patients [21].

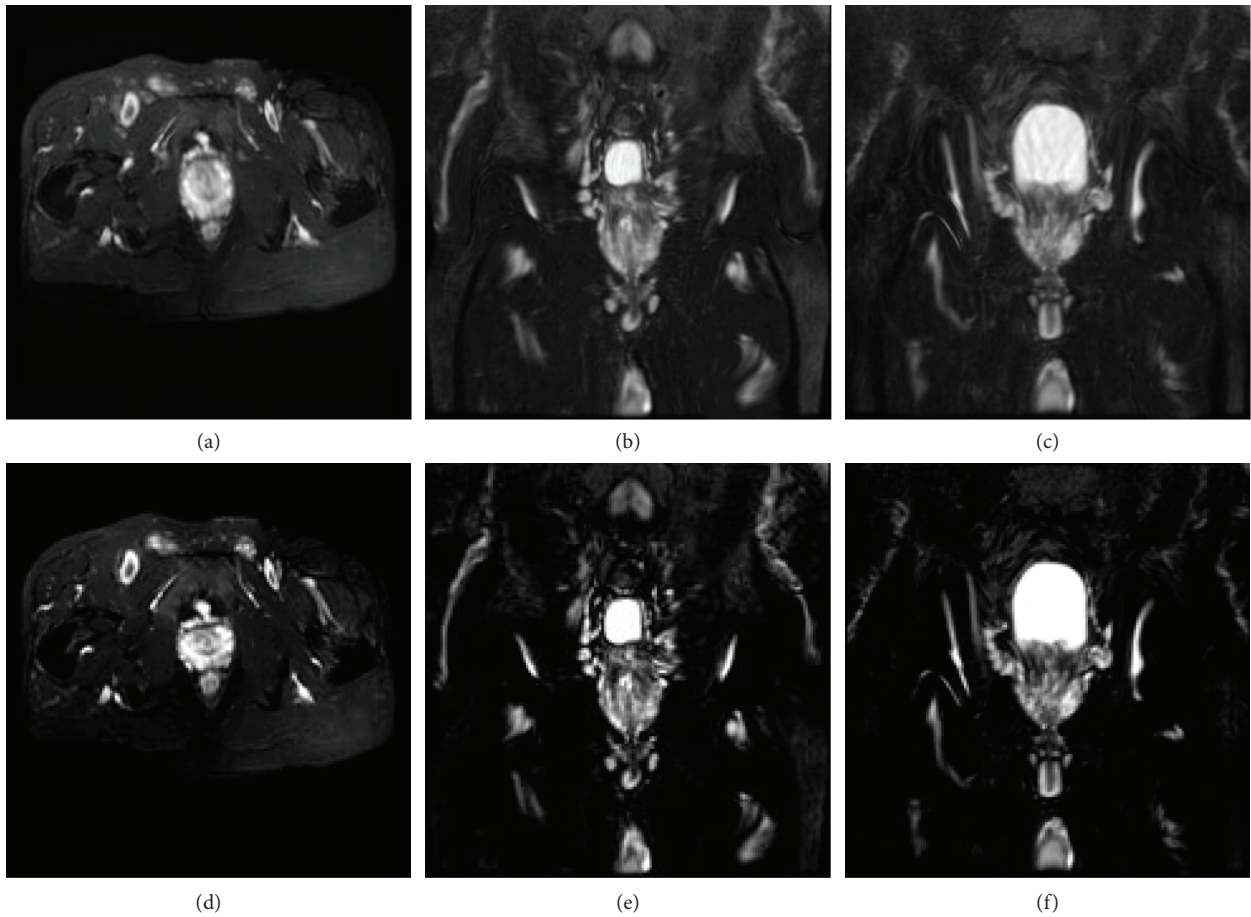


FIGURE 1: MRI images presentation of the typical case. (a)–(c): pre-processing image; (d)–(f): processed image.

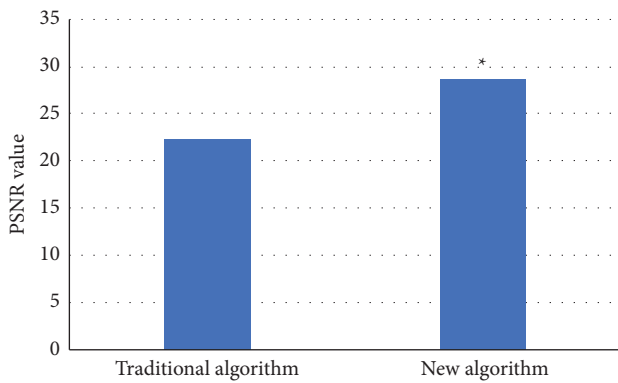


FIGURE 2: Comparison of PSNR index results. *Compared with traditional algorithm, $P < 0.05$.

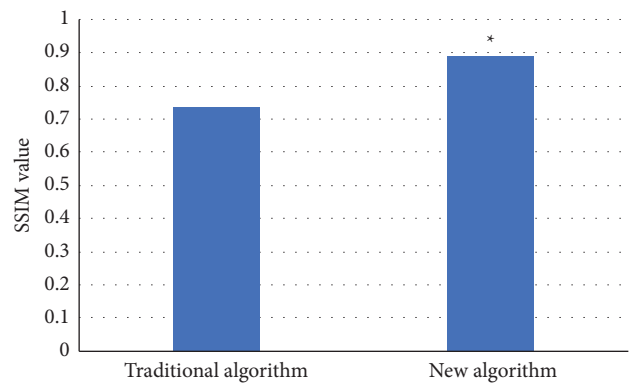


FIGURE 3: Comparison of SSIM index results. *Compared with traditional algorithm, $P < 0.05$.

MRI was used to diagnose PCa. The results showed that the negative predictive value, positive predictive value, accuracy, specificity, and sensitivity of PCa were 84.6%, 61.4%, 71.11%, 73.08%, and 61.9%, respectively. It can be found that its performance in PCa diagnosis is slightly better than in PSA diagnosis.

In recent years, computer and network technology have developed rapidly and advanced, gradually penetrating into various fields. It has also been applied and developed in the

medical field, and one of the more interesting technologies is super-resolution technology [22]. In the 1960s, high-resolution images can be obtained by mining the prior knowledge of low-resolution images and reconstructing image information for images with lower resolution. However, the results of further research show that the reconstructed image quality is interfered with greatly by noise and its quality is not high, so this algorithm has not been widely popularized and applied. After continuous

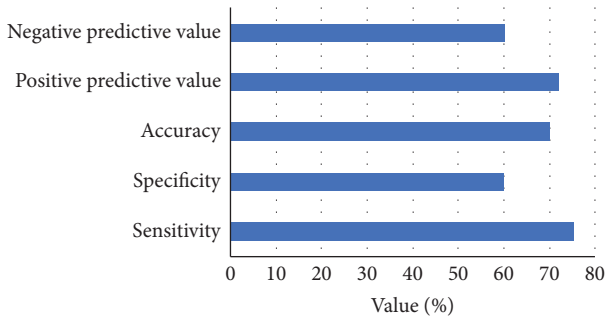


FIGURE 4: PSA diagnosis results.

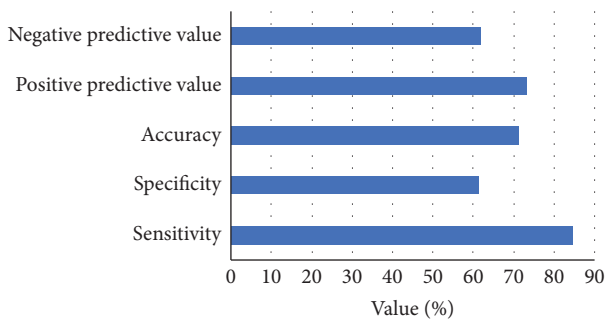


FIGURE 5: MRI diagnostic results.

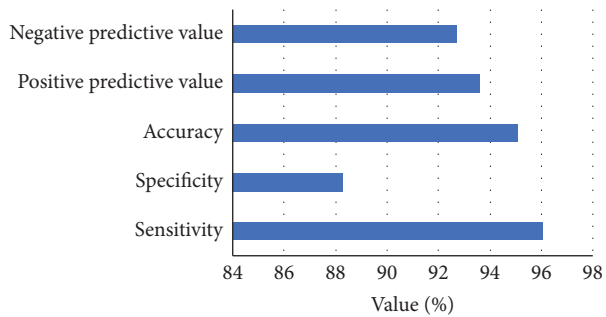
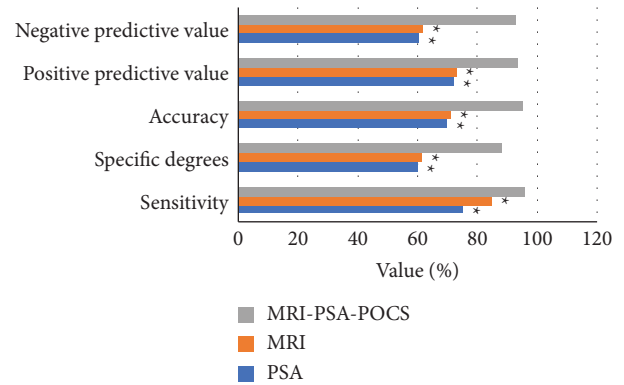


FIGURE 6: Diagnostic results of MRI combined with PSA based on super-resolution reconstruction algorithm.

development and progress, super-resolution technology has been continuously improved and innovated, of which the technology that has received more attention and higher performance is POCS [23]. The convergence speed of the algorithm is fast, and the image reconstruction time is greatly shortened. In recent years, there have also been many studies on the application of related technical medical fields. For example, some scholars use the POCS algorithm to input the super-resolution algorithm of cardiac images, and in the experiment, multiple low-resolution two-dimensional cardiac magnetic resonance images were reconstructed into three-dimensional super-resolution images, which can not only complete the reconstruction of cardiac magnetic resonance images but also be suitable for other human anatomical structures. There are many similar related studies, but there are few studies and analyses for PCa [24, 25]. MRI technology and the super-

FIGURE 7: Comparison of performance indicators of each method in the diagnosis of PCa. *Compared with MRI-PSA-POCS, $P < 0.05$.

resolution reconstruction algorithm were combined to diagnose PCa. The results showed that the negative predictive value, positive predictive value, accuracy, specificity, and sensitivity of PCa were 96.05%, 88.3%, 95.1%, 93.6%, and 92.7%, respectively. Its performance in PCa diagnosis is significantly better than PSA or MRI alone. This indicates that MRI technology based on the super-resolution reconstruction algorithm has high application value in PCa diagnosis. It provides a reference and a basis for clinical treatment of related diseases.

5. Conclusions

Prostate cancer patients were selected as the study subjects. All patients underwent PSA and MRI examinations. The obtained MRI images were processed by the super-resolution reconstruction algorithm. The PSNR and SSIM indexes were used to evaluate the image reconstruction performance of the algorithm. The accuracy, sensitivity, specificity, positive predictive value, and negative predictive value of PSA, MRI, and MRI combined with PSA based on the super-resolution reconstruction algorithm in the diagnosis of PCa were compared. The results show that the quality of the image processed by the super-resolution reconstruction algorithm was significantly improved, and the scores of PSNR and SSIM indexes of the proposed algorithm were significantly higher than those of the traditional image processing method. MRI combined with PSA based on the super-resolution reconstruction algorithm had significantly higher scores than PSA and MRI alone in the diagnosis of PCa. It provides a new idea and reference for the diagnosis of PCa in clinical practice. However, there are still some defects and deficiencies. The POCS algorithm was only introduced into MRI image processing of PCa patients. Moreover, more excellent algorithms are introduced, which makes it impossible to guarantee that the image processing algorithm is optimal. In the future, more algorithms will be introduced into MRI image processing of PCa patients in order to find the optimal image processing algorithm.

Data Availability

The data used to support the findings of this study are available from the corresponding author upon request.

Conflicts of Interest

The authors declare that they have no conflicts of interest.

References

- [1] J. K. Sehn, "Prostate cancer pathology: recent updates and controversies," *Missouri Medicine*, vol. 115, no. 2, pp. 151–155, 2018.
- [2] M. C. Haffner, W. Zwart, M. P. Roudier et al., "Genomic and phenotypic heterogeneity in prostate cancer," *Nature Reviews Urology*, vol. 18, no. 2, pp. 79–92, 2021.
- [3] H. Schatten, "Brief overview of prostate cancer statistics, grading, diagnosis and treatment strategies," *Advances in Experimental Medicine and Biology*, vol. 1095, pp. 1–14, 2018.
- [4] K. Komura, C. J. Sweeney, T. Inamoto, N. Ibuki, H. Azuma, and P. W. Kantoff, "Current treatment strategies for advanced prostate cancer," *International Journal of Urology*, vol. 25, no. 3, pp. 220–231, 2018.
- [5] M. Y. Teo, D. E. Rathkopf, and P. Kantoff, "Treatment of advanced prostate cancer," *Annual Review of Medicine*, vol. 70, pp. 479–499, 2019.
- [6] C. Ritch and M. Cookson, "Recent trends in the management of advanced prostate cancer," *F1000Research*, vol. 7, 2018.
- [7] T. Tsujino, K. Komura, T. Inamoto, and H. Azuma, "CRISPR screen contributes to novel target discovery in prostate cancer," *International Journal of Molecular Sciences*, vol. 22, no. 23, 2021.
- [8] M. Matsushita, K. Fujita, and N. Nonomura, "Influence of diet and nutrition on prostate cancer," *International Journal of Molecular Sciences*, vol. 21, no. 4, p. 1447, 2020.
- [9] D. Termini, D. J. Den Hartogh, A. Jaglanian, and E. Tsiani, "Curcumin against prostate cancer: current evidence," *Bio-molecules*, vol. 10, no. 11, p. 1536, 2020.
- [10] M. T. Vietri, G. D'Elia, G. Caliendo et al., "Hereditary prostate cancer: genes related, target therapy and prevention," *International Journal of Molecular Sciences*, vol. 22, no. 7, p. 3753, 2021.
- [11] C. DE Nunzio, F. Presicce, S. Giacinti, M. Bassanelli, and A. Tubaro, "Castration-resistance prostate cancer: what is in the pipeline?" *Minerva Urology and Nephrology*, vol. 70, no. 1, pp. 22–41, 2018.
- [12] X. Zhang, "Interactions between cancer cells and bone microenvironment promote bone metastasis in prostate cancer," *Cancer Communications*, vol. 39, no. 1, p. 76, 2019.
- [13] J. Mayor de Castro, J. Caño Velasco, J. Aragón Chamizo, G. Andrés Boville, F. Herranz Amo, and C. Hernández Fernández, "Cáncer de próstata localmente avanzado. Definición, diagnóstico y tratamiento (Locally advanced prostate cancer. Definition, diagnosis and treatment)," *Archivos Españoles de Urología*, vol. 71, no. 3, pp. 231–238, 2018.
- [14] C. C. Foster, R. R. Weichselbaum, and S. P. Pitroda, "Oligometastatic prostate cancer: reality or figment of imagination?" *Cancer*, vol. 125, no. 3, pp. 340–352, 2019.
- [15] T. Gourdin, "Recent progress in treating advanced prostate cancer," *Current Opinion in Oncology*, vol. 32, no. 3, pp. 210–215, 2020.
- [16] D. A. Siegel, M. E. O'Neil, T. B. Richards, N. F. Dowling, and H. K. Weir, "Prostate cancer incidence and survival, by stage and race/ethnicity—United States, 2001–2017," *MMWR Morb Mortal Wkly Rep*, vol. 69, no. 41, pp. 1473–1480, 2020.
- [17] M. Rosellini, M. Santoni, V. Mollica et al., "Treating prostate cancer by antibody-drug conjugates," *International Journal of Molecular Sciences*, vol. 22, no. 4, p. 1551, 2021.
- [18] T. Kimura and S. Egawa, "Epidemiology of prostate cancer in Asian countries," *International Journal of Urology*, vol. 25, no. 6, pp. 524–531, 2018.
- [19] K. M. Wheeler and M. A. Liss, "The microbiome and prostate cancer risk," *Current Urology Reports*, vol. 20, no. 10, p. 66, 2019.
- [20] A. Sokolova and H. Cheng, "Germline testing in prostate cancer: when and who to test," *Oncology*, vol. 35, no. 10, pp. 645–653, 2021.
- [21] F. Preisser, M. R. Cooperberg, J. Crook et al., "Intermediate-risk prostate cancer: stratification and management," *European Urology Oncology*, vol. 3, no. 3, pp. 270–280, 2020.
- [22] Z. Wan, Y. Dong, Z. Yu, H. Lv, and Z. Lv, "Semi-supervised support vector machine for digital twins based brain image fusion," *Frontiers in Neuroscience*, vol. 15, Article ID 705323, 2021.
- [23] P. C. Albertsen, "Prostate cancer screening and treatment: where have we come from and where are we going?" *BJU International*, vol. 126, no. 2, pp. 218–224, 2020.
- [24] S. Xie, Z. Yu, and Z. Lv, "Multi-disease prediction based on deep learning: a survey," *Computer Modeling in Engineering and Sciences*, vol. 128, no. 2, pp. 489–522, 2021.
- [25] J. L. Mohler and E. S. Antonarakis, "NCCN guidelines updates: management of prostate cancer," *Journal of the National Comprehensive Cancer Network*, vol. 17, no. 5.5, pp. 583–586, 2019.